

Temperature dependences of carbon assimilation processes in four dominant species from mountain grassland ecosystem

O. URBAN^{*,+†}, A. AČ^{*,++†}, J. KALINA^{**}, T. PRIWITZER^{***}, M. ŠPRTOVÁ^{*}, V. ŠPUNDA^{**}, and M.V. MAREK^{*,+++†}

*Laboratory of Plants Ecological Physiology, Institute of Systems Biology and Ecology,
Academy of Sciences of the Czech Republic, Poříčí 3b, 603 00 Brno, Czech Republic*

Department of Physics, Faculty of Science, Ostrava University, 30. dubna 22, 701 03 Ostrava 1, Czech Republic

National Forest Centre, Forest Research Institute, T.G. Masaryka 22, 960 92 Zvolen, Slovakia

Agricultural Faculty, University of South Bohemia, Studentská 13, 370 05 České Budějovice, Czech Republic

Institute of Physical Biology, University of South Bohemia, Zámek 136, 373 33 Nové Hrady, Czech Republic

Abstract

Temperature responses of carbon assimilation processes were studied in four dominant species from mountain grassland ecosystem, *i.e.* *Holcus mollis* (L.), *Hypericum maculatum* (Cr.), *Festuca rubra* (L.), and *Nardus stricta* (L.), using the gas exchange technique. Leaf temperature (T_L) of all species was adjusted within the range 13–30 °C using the Peltier thermoelectric cooler. The temperature responses of metabolic processes were subsequently modelled using the Arrhenius exponential function involving the temperature coefficient Q_{10} . The expected increase of global temperature led to a significant increase of dark respiration rate (R_D ; $Q_{10} = 2.0 \pm 0.5$), maximum carboxylation rate (V_{Cmax} ; $Q_{10} = 2.2 \pm 0.6$), and maximum electron transport rate (J_{max} ; $Q_{10} = 1.6 \pm 0.4$) in dominant species of mountain grassland ecosystems. Contrariwise, the ratio between J_{max} and V_{Cmax} linearly decreased with T_L [$y = -0.884 T_L + 5.24$; $r^2 = 0.78$]. Hence temperature did not control the ratio between intercellular and ambient CO₂ concentration, apparent quantum efficiency, and photon-saturated CO₂ assimilation rate (P_{max}). P_{max} primarily correlated with maximum stomatal conductance irrespective of T_L . Water use efficiency tended to decrease with T_L [$y = -0.21 T_L + 8.1$; $r^2 = 0.87$].

Additional key words: ambient and intercellular CO₂ concentrations; carboxylation rate; electron transport rate; photosynthesis; quantum efficiency; respiration; stomatal conductance; water use efficiency.

Introduction

With the predicted increase in global air temperature induced by the enhanced greenhouse effect, plant responses to increasing temperature have become a major part of the current eco-physiological research (Gunderson *et al.* 2000, Hikosaka *et al.* 2006), since the possible feedback of terrestrial ecosystems in terms of altered CO₂ sink capacity possess large uncertainty in climate models (Cox *et al.* 2000). Temperature affects metabolic processes *via* influences on the chemical reaction kinetics and on the effectiveness of the various enzymes involved.

A widely applied empirical approach describing the temperature response of physiological processes is based on the observation that a given temperature increment increases the reaction rate k by a constant factor (Johnson and Thornley 1985, Hikosaka 1997):

$$k = k_r Q_{10}^{\frac{T-T_r}{10}}, \quad (1)$$

where k_r is the rate constant of physiological process at the reference temperature T_r , and Q_{10} is the factor by

Received 19 October 2006, accepted 26 February 2007.

[†]Corresponding author; fax: +420 – 543211560, e-mail: otmar@brno.cas.cz

Abbreviations: *AQE* – apparent quantum efficiency; C_a (C_i) – ambient (intercellular) CO₂ concentration; *Chl* (*Car*) – chlorophyll (carotenoid); *DM* – dry mass; E_{max} – maximum transpiration rate; *FM* – fresh mass; g_{smax} – maximum stomatal conductance; J_{max} – maximum electron transport rate; P (P_{max}) – (maximum) CO₂ assimilation rate; *PPFD* – photosynthetic photon flux density; Q_{10} – factor by which the rate constant increases for a 10 °C temperature increment; R_D – dark respiration rate; *RuBP* – ribulose-1,5-bisphosphate; *RUBPCO* – ribulose-1,5-bisphosphate carboxylase/oxygenase; *RWC* – relative water content; *SLA* – specific leaf area; T_L – leaf temperature; V_{Cmax} – maximum carboxylation rate; *VPD* – vapour pressure deficit; *WUE* – water use efficiency.

Acknowledgement: The work forms a part of the research supported by the grants no. EVK2-CT-2001-000125 (EU), OC 627.001 (Ministry of Education of the Czech Republic), by CzechCarbo project VaV 640/18/03 (Ministry of Environmental Protection), and by the ISBE AS CR research intention AV0Z60870520.

which the rate constant increases for a 10 °C temperature increment. The Q_{10} temperature coefficient is constant only in a narrow range of temperatures 1.40–2.00 for most of enzyme reactions and 1.03–1.30 for physical processes (Larcher 2003). Therefore, the Q_{10} of metabolic processes varies with temperature. At low temperatures it is large, for as a rule enzyme reactions are rate-limiting, whereas at higher temperatures it decreases because physical processes (e.g. diffusion velocity) become limiting (Larcher 2003).

In the biochemical model of C_3 photosynthesis, the CO_2 assimilation rate (P) is limited either by the carboxylation activity of ribulose-1,5-bisphosphate carboxylase/oxygenase (RuBPCO) enzyme or by the ribulose-1,5-bisphosphate (RuBP) regeneration (Farquhar *et al.* 1980, Makino and Mae 1999). The limiting step is different depending on the CO_2 concentration. At low CO_2 concentrations [$<200 \mu\text{mol}(CO_2) \text{ mol}^{-1}$], RuBP pool is saturated and the limiting step of photosynthesis is carboxylation of RuBP. The CO_2 assimilation rate (P_c) is expressed as a function of intercellular CO_2 concentration (C_i):

$$P_c = \frac{V_{C_{\max}} (C_i - \Gamma^*)}{C_i + K_c (1 + O/K_o)} \quad (2)$$

where $V_{C_{\max}}$ is the maximum carboxylation rate by RuBPCO, K_c and K_o are the Michaelis-Menten constants of RuBPCO for CO_2 and O_2 , respectively, O is the O_2 concentration, and Γ^* is the CO_2 compensation concentration in the absence of day respiration.

Contrariwise, at high CO_2 concentrations the CO_2 assimilation rate (P_j) is limited by RuBP regeneration. Under photon energy-saturated conditions, P_j is expressed as

$$P_j = \frac{J_{\max} (C_i - \Gamma^*)}{4 C_i + 8 \Gamma^*} \quad (3)$$

where J_{\max} is the maximum rate of RuBP regeneration estimated as the rate of electron transport. The RuBP regeneration process involves electron transport, ATP synthesis, and Calvin cycle processes other than carboxylation.

Temperature dependence of these parameters is fitted using (a) Arrhenius model (k is the function of the activation energy, E_a) or (b) models with temperature optimum (k is the function of E_a , variation of the enthalpy, ΔH , and the entropy, ΔS) (Johnson and Thornley 1985).

With changes in growth temperature, many plants show considerable plasticity in their assimilation characteristics. The temperature acclimation of photosynthesis greatly varies among the plant species (Yamasaki *et al.* 2002). For example, plants grown at low temperatures have lower temperature optimum for photosynthesis comparing to plants grown at higher temperatures (Berry and Björkman 1980). Many studies assume that K_c , K_o , and Γ^* are not affected by growth conditions and are not species dependent. Variability in the temperature dependence of P is thus ascribed to changes in (1) intercellular CO_2 concentration, C_i , (2) activation energy of $V_{C_{\max}}$, (3) activation energy of J_{\max} , and (4) the ratio of J_{\max} to $V_{C_{\max}}$ (Farquhar *et al.* 1980, Makino and Mae 1999, Hikosaka *et al.* 2006).

Objectives of our study were (a) to describe the variability of assimilation characteristics of dominant species from mountain grassland ecosystem, (b) to characterize the temperature dependences of main assimilation characteristics, and (c) to discuss the potential contribution of the above mentioned factors to the assimilation-temperature response curve.

Materials and methods

Site: The grass stand, 3.5 ha in size, is situated on the experimental research site Bílý Kříž (Beskydy Mts., 49°33'N, 18°32'E, NE of the Czech Republic, 825–860 m a.s.l.) and it forms a part of the IP CARBOEUROPE and CARBOMONT networks. This area is characterised as cool (annual mean temperature 5.5 °C) and humid (annual mean relative air humidity 80 %) with high precipitation (annual amount 1 000–1 400 mm). Soil type according to FAO is Ferric Podzols [parent material: mesozoic Godula sandstone (flysch type); soil texture: loamy/sand-loamy with 30–40 % of gravel]. Soil depth is 60–80 cm. The grass stand is divided into unmanaged (association *Molinio-Arrhenatheretea*, class *Polygono-Trisetion*) and managed (association *Nardo-Callunetea*, class *Nardo-Agrostion tenuis*) parts. Unmanaged stand was neither cut nor fertilised over the last ten years, managed stand is cut once a year (end of July).

Fully developed sun exposed leaves (second leaf from the top of the plant) of *Holcus mollis* (L.), *Hypericum maculatum* (Cr.) (from unmanaged part of the grass stand) and *Festuca rubra* (L.), *Nardus stricta* (L.) (from managed part of the grass stand) were investigated in the middle of June. All samples were measured *in situ* under similar weather conditions within the range of 5 d.

Gas exchange: An open portable photosynthetic system with infra-red gas analyser *Li-6400* (Li-Cor, USA) was used for *in situ* measurement of the relationships between CO_2 assimilation rate and incident photosynthetic photon flux density ($P\text{-PPFD}$) and intercellular CO_2 concentration ($P\text{-}C_i$). The $P\text{-PPFD}$ response curve was measured under the constant ambient CO_2 concentration [$370 \pm 5 \mu\text{mol}(CO_2) \text{ mol}^{-1}$] and the predetermined set of PPFDs (0, 25, 50, 100, 200, 400, 800, 1 200, and 1 500 $\mu\text{mol m}^{-2} \text{ s}^{-1}$) using a red-blue LED light source

Li-6400-02B (*Li-COR*, USA). P -PPFD response curves were then fitted by a non-rectangular hyperbola (Prioul and Chartier 1977) and thus the maximum assimilation rate (P_{\max}) at saturating PPFD, apparent quantum efficiency (AQE), and dark respiration rate (R_D) were determined.

The P - C_i response curve was produced starting at an ambient CO_2 concentration (C_a) of 370 $\mu\text{mol}(\text{CO}_2) \text{ mol}^{-1}$ and decreased stepwise to 50 $\mu\text{mol}(\text{CO}_2) \text{ mol}^{-1}$, and then increasing to 1 500 $\mu\text{mol}(\text{CO}_2) \text{ mol}^{-1}$. PPFD was maintained at 1 500 $\mu\text{mol}(\text{CO}_2) \text{ mol}^{-1}$ using the *Li-6400-02B* light source (*Li-Cor*, USA). Values of P - C_i response curves were used to estimate assimilation capacity under saturating PPFD and CO_2 concentration (P_{sat}), maximal carboxylation rate (V_{Cmax}), and maximal electron transport rate (J_{\max}) using Eqs. 2 and 3 (Farquhar *et al.* 1980).

Microclimatic conditions inside the assimilation chamber were kept constant during the above described measurements of P -PPFD and P - C_i responses (leaf temperature T_L 20±1 °C, relative air humidity 60±3 %). Subsequently, T_L was adjusted within the interval of

13–30 °C (*i.e.* 13, 15, 20, 25, and 30 °C) using the Peltier thermoelectric cooler to determine the temperature dependencies of above mentioned parameters. The temperature responses were modelled using the Eq. 1 (Johnson and Thornley 1985).

Plant pigments from dark-adapted (30 min) and liquid nitrogen frozen leaf segments (*ca.* 100 mg of fresh mass, FM) were extracted with 80 % acetone and a small amount of MgCO_3 . The supernatant obtained after centrifugation at 480×g for 3 min was used for spectrophotometric (*UV-VIS 550, Unicam, U.K.*) estimation of chlorophyll (Chl) *a* and *b* and total carotenoid (Car) contents (Lichtenthaler 1987). FM (*Sartorius, Japan*) and projected leaf area (Portable Area Meter, *Li-3000A, Li-Cor, USA*) were determined in the parallel samples. Subsequently, leaves were oven-dried at 80 °C for 48 h for dry mass (DM) determination. Specific leaf area (SLA), *i.e.* projected leaf area/leaf DM, and relative water content (RWC), *i.e.* (leaf FM – leaf DM)/leaf FM [%], were calculated.

Results

The selected CO_2 assimilation characteristics of all investigated species at T_L of 20 °C are presented in Fig. 1 and Table 1. Variations in P reflect differences in whole leaf structure (SLA, RWC, and pigments) (Table 2), as well as leaf N status and adaptation to PPFD.

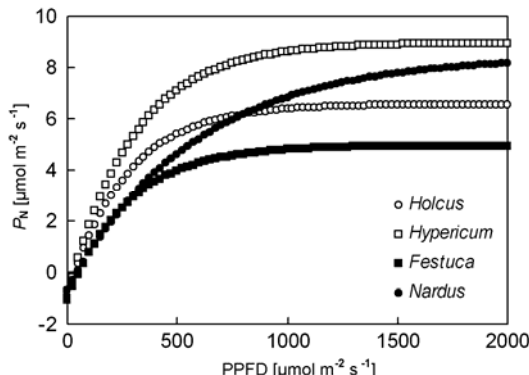


Fig. 1. The mean relationships between CO_2 assimilation rate (P) and incident photosynthetic photon flux density (PPFD) of investigated plant species *Holcus mollis* (empty circles), *Hypericum maculatum* (empty squares), *Festuca rubra* (filled squares), and *Nardus stricta* (filled circles). All measurements were done on sun exposed leaves at leaf temperature of 20 °C. Means of 4 measurements per species.

Discussion

Under natural conditions, variability of grasslands results from externally generated factors (*i.e.* those affecting vegetation, but not affected by it, *e.g.* depth of soil, incoming PPFD, growth temperature, *etc.*) and internally generated factors (*i.e.* factors affected by vegetation, such

T_L did not influence C_i/C_a ; these values ranged between 0.72 (at 20 °C) and 0.77 (at 15 °C) for *H. mollis* (Fig. 2A). Mean C_i/C_a obtained by averaging data through the whole interval of temperatures was 0.89 for *N. stricta*, 0.87 for *F. rubra*, 0.85 for *H. maculatum*, and 0.75 for *H. mollis* (Fig. 2B). Increase of T_L led to an exponential increase of V_{Cmax} ($r^2 = 0.74$) and J_{\max} ($r^2 = 0.51$). Also R_D tightly correlated with T_L according to an exponential function ($r^2 = 0.77$). Q_{10} was 2.2±0.66, 1.6±0.41, and 2.0±0.5 for V_{Cmax} , J_{\max} , and R_D , respectively (Fig. 3A, B, C). The Q_{10} values of individual species are shown in Table 2. The rate constants of these physiological processes at T_L of 20 °C correspond to the values presented in Table 1. Contrariwise, the temperature responses of P_{\max} (Fig. 3D) and AQE (data not shown) between 13 and 30 °C did not suggest a clear temperature dependence.

P_{\max} correlated with g_{smax} (Fig. 4). Since all measurements of assimilation characteristics were done under constant vapour pressure deficit (VPD = 1.2±0.2 kPa), g_{smax} did not show any correlation with T_L .

WUE at saturating irradiance (PPFD >1 200 $\mu\text{mol m}^{-2} \text{ s}^{-1}$), calculated as the ratio between P_{\max} and maximum transpiration rate (E_{\max}), linearly decreased with increasing T_L (Fig. 5A). This phenomenon was caused by significant increase of E_{\max} with increasing T_L (Fig. 5B).

as horizontal radiation variation or nutrient availability (Larcher 2003). The variability of the CO_2 assimilation parameters is strongly affected by pigment composition (Lichtenthaler 1987), leaf structure (Reich *et al.* 1998), leaf nitrogen content (Evans 1989), and by leaf actual and

growth temperature (Berry and Björkman 1980, Hikosaka *et al.* 2006). In the literature, changes in the temperature dependence of P are ascribed to changes in C_i , activation energy of $V_{C\max}$, activation energy of J_{\max} , and the ratio of J_{\max} to $V_{C\max}$ (Farquhar *et al.* 1980, Makino and Mae 1999, Hikosaka *et al.* 2006).

Effect of temperature on C_i : Temperature dependence of C_i potentially affects the temperature dependence of photosynthesis. The optimal temperature is low if C_i decreases with increasing T_L (Hikosaka *et al.* 2006). We demonstrated that C_i/C_a is independent on T_L (Fig. 2A), but some studies show that C_i/C_a ratio is changing during the day (Marek and Pirochová 1990) and it decreases with increasing T_L (Ferrar *et al.* 1989). Furthermore, g_s is more sensitive to vapour pressure deficit (VPD) rather than to temperature or relative air humidity (Aphalo and Jarvis 1991). For example, Leuning (1995) suggested that g_s is regulated in order to maintain the C_i/C_a ratio constant, irrespective of temperature under constant VPD.

However, VPD increases with T_L under natural field conditions, which may decrease C_i .

Changes of C_i/C_a are pivotal to the application of the models simulating WUE of stands under dynamically changing field environments (Xu and Hsiao 2004). Our finding that WUE linearly decreases with increase of T_L (Fig. 5A) is in accordance with field experiments of Joshi and Palni (2005) on *Hordeum himalayens* and *H. vulgare*. However, Zhang *et al.* (2001) reported that WUE varies inversely with leaf temperature following a hyperbolic function. Allen *et al.* (2003) demonstrated that mean daily evapotranspiration rate of *Glycine max* plants was linearly related to mean air temperature (T_{air}) and whole-day WUE declined linearly with T_{air} with a slope of $-0.150 \text{ } \mu\text{mol}(\text{CO}_2) \text{ mmol}^{-1}(\text{H}_2\text{O}) \text{ } ^\circ\text{C}^{-1}$. Changes in evapotranspiration rate and WUE were governed by changes in T_L and canopy resistance (Allen *et al.* 2003).

Temperature dependence of RuBPCO-limited photosynthesis: *In vitro* RuBPCO activity at saturating CO_2

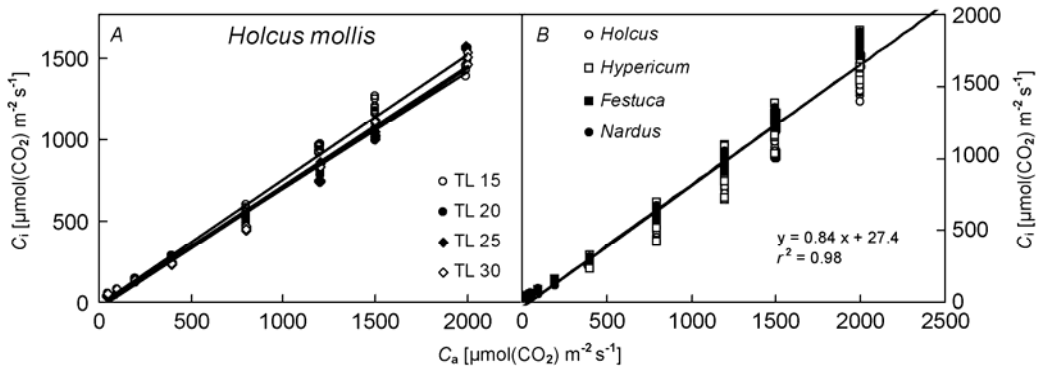


Fig. 2. Intercellular CO_2 concentration (C_i) in relation to ambient CO_2 concentration (C_a) in (A) *Holcus mollis* under the predetermined set of leaf temperatures (T_L) and (B) in all investigated plant species and whole T_L interval. The slopes of linear regressions in (A) yielded 0.77 for $T_L = 15$ °C, 0.72 for 20 °C, 0.73 for 25 °C, and 0.74 for 30 °C with r^2 between 0.96 and 0.98. In (B), the mean slopes of individual species yielded 0.75 for *Holcus mollis*, 0.85 for *Hypericum maculatum*, 0.87 for *Festuca rubra*, and 0.89 for *Nardus stricta*, with r^2 between 0.96 and 0.99. Linear regression of all data is presented in (B).

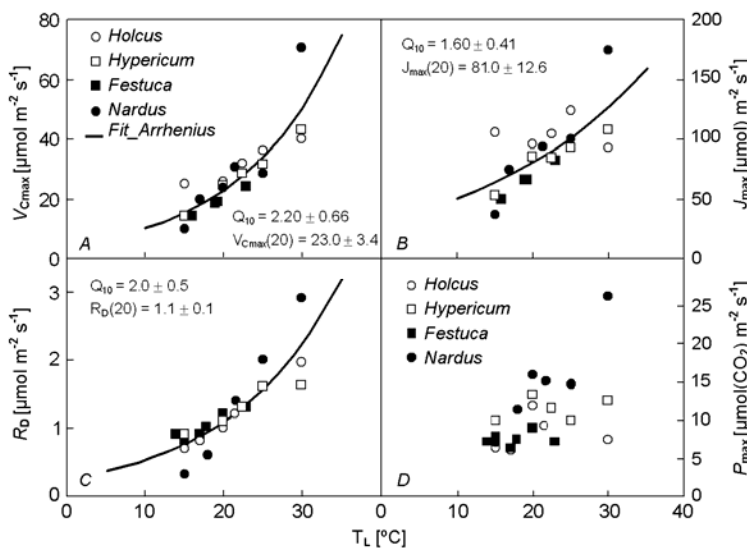


Fig. 3. Temperature dependencies of (A) maximum assimilation rate at saturating PPFD (P_{\max}), (B) dark (mitochondrial) respiration (R_D), (C) maximum carboxylation rate ($V_{C\max}$), and (D) maximum electron transport rate (J_{\max}) estimated by gas-exchange technique. The Arrhenius exponential function (Eq. 1) was fitted to the data (Fit_Arrhenius). Means \pm standard deviations of Q_{10} and the rate constant of physiological process at the reference temperature 20 °C are presented in (B,C,D); $n = 16$.

Table 1. Means \pm standard deviations of selected physiological parameters derived from the relationships between CO_2 assimilation rate (P) and incident photosynthetic photon flux density (PPFD) or intercellular CO_2 concentration (C_i) estimated at leaf temperature of 20 °C. R_D – dark respiration [$\mu\text{mol}(\text{CO}_2) \text{ m}^{-2} \text{ s}^{-1}$], AQE – apparent quantum efficiency [$\text{mol}(\text{CO}_2) \text{ mol}^{-1}(\text{photon})$], P_{\max} – maximum assimilation rate at saturating PPFD [$\mu\text{mol}(\text{CO}_2) \text{ m}^{-2} \text{ s}^{-1}$], g_{\max} – maximum stomatal conductance at saturating PPFD [$\text{mmol}(\text{H}_2\text{O}) \text{ m}^{-2} \text{ s}^{-1}$], E_{\max} – maximum transpiration rate at saturating PPFD [$\mu\text{mol}(\text{H}_2\text{O}) \text{ m}^{-2} \text{ s}^{-1}$], P_{sat} – saturated assimilation rate at saturating PPFD and C_i [$\mu\text{mol}(\text{CO}_2) \text{ m}^{-2} \text{ s}^{-1}$], V_{Cmax} – maximum carboxylation rate [$\mu\text{mol}(\text{CO}_2) \text{ m}^{-2} \text{ s}^{-1}$], J_{\max} – maximum electron transport rate [$\mu\text{mol}(\text{electron}) \text{ m}^{-2} \text{ s}^{-1}$]. Means of 4 measurements per species.

	P-PPFD			$P-C_i$				
	R_D	AQE	P_{\max}	g_{\max}	E_{\max}	P_{sat}	V_{Cmax}	J_{\max}
<i>Holcus mollis</i>	1.00 \pm 0.20	0.039 \pm 0.006	12.0 \pm 1.0	0.13 \pm 0.01	2.0 \pm 0.2	21.0 \pm 2.0	26.0 \pm 1.0	96.0 \pm 12.3
<i>Hypericum maculatum</i>	1.10 \pm 0.15	0.033 \pm 0.003	10.0 \pm 1.5	0.19 \pm 0.01	3.5 \pm 0.3	18.0 \pm 1.7	25.0 \pm 3.3	85.0 \pm 9.2
<i>Festuca rubra</i>	1.20 \pm 0.18	0.024 \pm 0.002	8.8 \pm 0.8	0.14 \pm 0.01	1.7 \pm 0.1	14.0 \pm 1.2	18.0 \pm 1.0	66.0 \pm 3.0
<i>Nardus stricta</i>	1.40 \pm 0.95	0.015 \pm 0.007	16.0 \pm 1.4	0.22 \pm 0.01	2.2 \pm 0.3	19.0 \pm 2.1	22.0 \pm 2.3	84.0 \pm 10.6

Table 2. Means \pm standard deviations of contents of chlorophyll (Chl) $a+b$ and total carotenoids (Car) [$\text{g kg}^{-1}(\text{DM})$], Chl a/b , specific leaf area (SLA = projected leaf area/leaf DM) [$\text{m}^2 \text{ kg}^{-1}(\text{DM})$], relative water content (RWC) [%], and temperature coefficient Q_{10} of dark respiration (R_D), maximum carboxylation rate (V_{Cmax}), and maximum electron transport rate (J_{\max}) in leaves of studied species. $n = 8$ or 4–5 (Q_{10}).

	Chl ($a+b$)	Car	Chl a/b	SLA	RWC	Q_{10}	V_{Cmax}	J_{\max}
	R_D							
<i>Holcus mollis</i>	4.10 \pm 0.52	1.20 \pm 0.10	3.10 \pm 0.06	28.0 \pm 1.4	69.0 \pm 0.4	1.9 \pm 0.2	1.4 \pm 0.1	1.0 \pm 0.2
<i>Hypericum maculatum</i>	6.80 \pm 0.95	1.70 \pm 0.10	2.90 \pm 0.13	23.0 \pm 4.0	65.0 \pm 1.9	1.5 \pm 0.2	1.9 \pm 0.1	1.5 \pm 0.1
<i>Festuca rubra</i>	3.90 \pm 0.29	0.60 \pm 0.04	2.70 \pm 0.06	10.0 \pm 1.3	58.0 \pm 4.3	1.7 \pm 0.2	2.1 \pm 0.2	1.9 \pm 0.2
<i>Nardus stricta</i>	3.90 \pm 0.29	0.80 \pm 0.05	2.80 \pm 0.10	7.0 \pm 0.9	53.0 \pm 5.2	2.9 \pm 0.3	3.2 \pm 0.2	2.2 \pm 0.2

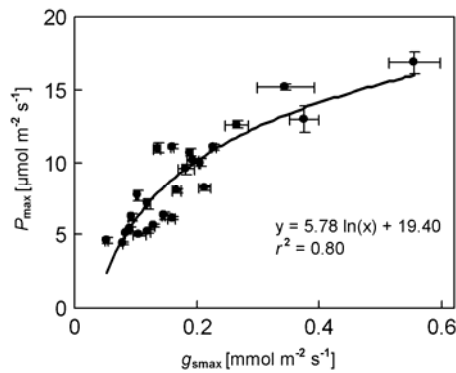


Fig. 4. Relationship between maximum CO_2 assimilation rate (P_{\max}) and maximum stomatal conductance (g_{\max}). Means (4 leaves per species) at constant temperature; bars represent standard deviations. The logarithmic function was fitted to the data.

exponentially increases with temperature (Jordan and Ogren 1984). Similarly to our results (Fig. 3A), in many plant species V_{Cmax} determined at a leaf-level exponentially increases from 15 to 30 °C, but the deactivation is often substantial at very high temperature (Wohlfahrt *et al.* 1999, Hikosaka *et al.* 2006).

Several mechanisms may be involved in the change of activation energy of V_{Cmax} . The first one is internal CO_2 conductance. Bernacchi *et al.* (2001) determined the temperature dependence of internal CO_2 conductance in tobacco (*Nicotiana tabacum*) leaves, which increased

with rising temperature with Q_{10} of 2.2 and had a maximum at 35.0–37.5 °C. Therefore, P above T_L of

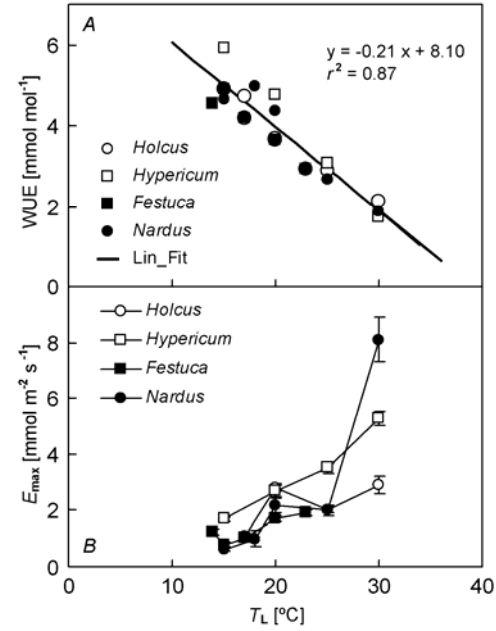


Fig. 5. Effects of leaf temperature (T_L) on (A) water use efficiency (WUE) and (B) transpiration rate (E_{\max}) under saturating photosynthetic photon flux density (PPFD > 1 200 $\mu\text{mol m}^{-2} \text{ s}^{-1}$). Means (4 leaves per species) at constant temperature; bars represent standard deviations. Linear regression of all data (Lin_Fit) is presented in (A).

40 °C may be suppressed by a lowered chloroplast CO₂ concentration. The second mechanism is the activation state of RuBPCO. The activation state of RuBPCO decreases at high temperature. Crafts-Brandner and Salvucci (2000) showed that when T_L exceeded 35 °C, P in cotton was lower than expected from RuBPCO kinetics. Inactivation of RuBPCO at high temperature may involve a decrease in activity of RuBPCO activase and an increase in the synthesis of xylulose-1,5-bisphosphate, which inactivates RuBPCO (Salvucci and Crafts-Brandner 2004).

Temperature dependence of RuBP regeneration-limited photosynthesis: The favourable T_L allowing 90–100 % of the highest P in *Quercus ilex* were 14–28 °C, decreasing over 50 % when T_L values were, respectively, below 6 °C and over 37 °C (Gratani *et al.* 2000). This temperature response of J_{\max} has usually been modelled by a modified Arrhenius type of exponential equation. However, deactivation of J_{\max} occurs at high temperature in many species (June *et al.* 2004). A shift in the optimal temperature for apparent J_{\max} , caused by growth temperature, was observed in some species, but not in the other ones (reviewed in June *et al.* 2004, Hikosaka *et al.* 2006).

Changes in the heat tolerance in components of the RuBP regeneration process have been shown by many

studies. Badger *et al.* (1982) showed that the thermal stability of various Calvin cycle enzymes is changing with growth temperature. Studies using Chl fluorescence analysis have shown that the thermostability of photosystem 2 changes with growth temperature (Berry and Björkman 1980). However, it is still unclear which components determine the temperature dependence of J_{\max} .

Balance between carboxylation and regeneration of RuBP: V_{Cmax} and J_{\max} were linearly correlated (Fig. 6A). A strong correlation between J_{\max} and V_{Cmax} , based on a literature survey of 109 species (Wullschleger 1993) suggests relatively constant balance between carboxylation and regeneration of RuBP, irrespective of species and growth conditions. Leuning (1997) improved this relationship by scaling it to a temperature of 20 °C, suggesting certain temperature influence. Also Wohlfahrt *et al.* (1999) demonstrated at 20 °C a similar linear relationship between J_{\max} and V_{Cmax} in sun leaves of 30 species from differently managed mountain grassland ecosystems. The differences were assigned to variations in their N use efficiency. Moreover, our data document that the ratio of J_{\max} to V_{Cmax} linearly decreased with T_L increase (Fig. 6B). It was caused by different temperature dependence of V_{Cmax} and J_{\max} (see Fig. 3A,B and Q_{10} in Table 2).

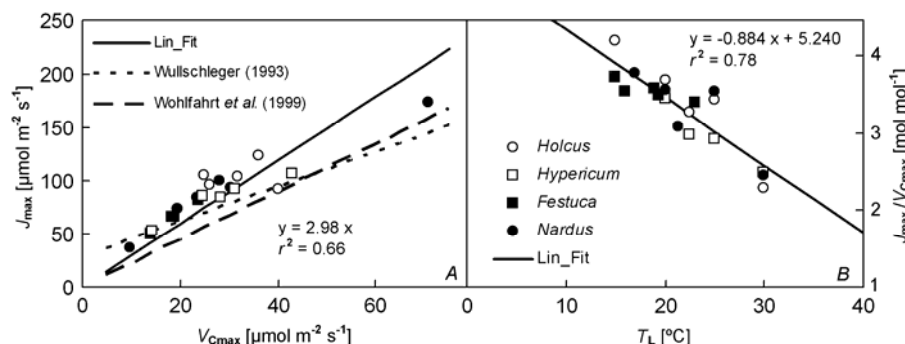


Fig. 6. (A) Relationship between the maximum rate of carboxylation (V_{Cmax}) and the maximum rate of electron transport (J_{\max}) as calculated from P - C_i curves under saturating photosynthetic photon flux density (PPFD = 1 500 $\mu\text{mol m}^{-2} \text{s}^{-1}$). The solid line represents the linear regression of data (Lin_Fit) in this study, the dotted line ($J_{\max} = 29.1 + 1.64 V_{\text{Cmax}}$) represents the relationship of Wullschleger (1993) from 109 C₃ plant species, and the dashed line ($J_{\max} = 2.312 V_{\text{Cmax}}$) represents the relationship of 30 species from mountain grassland ecosystems at a reference temperature of 20 °C (Wohlfahrt *et al.* 1999). (B) Relationship between leaf temperature (T_L) and J_{\max} to V_{Cmax} (J_{\max}/V_{Cmax}). In both (A, B), symbols represent mean values (4 leaves per species) at given temperature.

Hikosaka *et al.* (1999) showed that *Quercus myrsinifolia* alters the J_{\max} to V_{Cmax} ratio depending on the growth temperature. When the plants are grown at high temperature, P at 350 $\mu\text{mol}(\text{CO}_2) \text{ mol}^{-1}$ was limited by RuBP carboxylation above 22 °C and by RuBP regeneration below 22 °C, while it was limited by RuBP carboxylation at any temperature in plants grown at low temperature. Similar changes in the J_{\max} to V_{Cmax} ratio were observed in *Polygonum cuspidatum*, spinach, and *Plantago asiatica* (reviewed in Hikosaka *et al.* 2006). However, there are also many annual species that did not

show growth temperature-dependent changes in the J_{\max} to V_{Cmax} ratio (e.g. Bunce 2000). Hikosaka (1997) presented the hypothesis that if the temperature dependence of P_C and P_J are similar, a change in the J_{\max} to V_{Cmax} ratio does not alter the temperature dependence of photosynthesis.

We conclude that the expected increase of temperature leads to a significant increase of R_D ($Q_{10} = 2.0 \pm 0.5$) and maximum V_{Cmax} ($Q_{10} = 2.2 \pm 0.6$) in dominant species of mountain grassland ecosystems. Contrariwise, the ratio J_{\max}/V_{Cmax} linearly decreases with leaf temperature

[$y = -0.884T_L + 5.24$; $r^2 = 0.78$]. Our results support the hypothesis that temperature does not control C_i/C_a , AQE, and P_{\max} . PPFD-saturated CO₂ assimilation rate primarily

correlates with $g_{s\max}$. Finally, our data suggest that WUE tends to decrease with T_L [$y = -0.21T_L + 8.1$; $r^2 = 0.87$].

References

Allen, L.H., Pan, D.Y., Boote, K.J., Pickering, N.B., Jones, J.W.: Carbon dioxide and temperature effects on evapotranspiration and water use efficiency of soybean. – *Agron. J.* **95**: 1071-1081, 2003.

Aphalo, P.J., Jarvis, P.G.: Do stomata respond to relative humidity? – *Plant Cell Environ.* **14**: 127-132, 1991.

Badger, M.R., Björkman, O., Armond, P.A.: An analysis of photosynthetic response and adaptation to temperature in higher plants: temperature acclimation in the desert evergreen *Nerium oleander* L. – *Plant Cell Environ.* **5**: 85-99, 1982.

Bernacchi, C.J., Singsaas, E.L., Pimentel, C., Portis, A.R., Jr., Long, S.P.: Improved temperature response functions for models of Rubisco-limited photosynthesis. – *Plant Cell Environ.* **24**: 253-259, 2001.

Berry, J., Björkman, O.: Photosynthetic response and adaptation to temperature in higher plants. – *Annu. Rev. Plant Physiol.* **31**: 491-543, 1980.

Bunce, J.A.: Acclimation of photosynthesis to temperature in eight cool and warm climate herbaceous C₃ species: Temperature dependence of parameters of a biochemical photosynthesis model. – *Photosynth. Res.* **63**: 59-67, 2000.

Cox, P.M., Betts, R.A., Jones, C.D., Spall, S.A., Totterdell, I.J.: Acceleration of global warming due to carbon-cycle feedbacks in a coupled climate model. – *Nature* **408**: 184-187, 2000.

Crafts-Brandner, S.J., Salvucci, M.E.: Rubisco activase constrains the photosynthetic potential of leaves at high temperature and CO₂. – *Proc. nat. Acad. Sci. USA* **97**: 13430-13435, 2000.

Evans, J.R.: Photosynthesis and nitrogen relationships in leaves of C₃ plants. – *Oecologia* **78**: 9-19, 1989.

Farquhar, G.D., Caemmerer, S. von, Berry, J.A.: A biochemical model of photosynthetic CO₂ assimilation in leaves of C₃ species. – *Planta* **149**: 78-90, 1980.

Ferrar, P.J., Slatyer, R.O., Vranjic, J.A.: Photosynthetic temperature acclimation in *Eucalyptus* species from diverse habitats and a comparison with *Nerium oleander*. – *Aust. J. Plant Physiol.* **16**: 199-217, 1989.

Gratani, L., Pesoli, P., Crescente, M.F., Aichner, K., Larcher, W.: Photosynthesis as a temperature indicator in *Quercus ilex* L. – *Global Planet. Change* **24**: 153-163, 2000.

Gunderson, C.A., Norby, R.J., Wullschleger, S.D.: Acclimation of photosynthesis and respiration to simulated climatic warming in northern and southern populations of *Acer saccharum*: laboratory and field evidence. – *Tree Physiol.* **20**: 87-95, 2000.

Hikosaka, K.: Modelling optimal temperature acclimation of the photosynthetic apparatus in C₃ plants with respect to nitrogen use. – *Ann. Bot.* **80**: 721-730, 1997.

Hikosaka, K., Ishikawa, K., Borjigidai, A., Muller, O., Onoda, Y.: Temperature acclimation of photosynthesis: mechanisms involved in the changes in temperature dependence of photosynthetic rate. – *J. exp. Bot.* **57**: 291-302, 2006.

Hikosaka, K., Murakami, A., Hirose, T.: Balancing carboxylation and regeneration of ribulose-1,5-bisphosphate in leaf photosynthesis in temperature acclimation of an evergreen tree, *Quercus myrsinaefolia*. – *Plant Cell Environ.* **22**: 841-849, 1999.

Johnson, I.R., Thornley, J.H.M.: Temperature dependence of plant and crop processes. – *Ann. Bot.* **55**: 1-24, 1985.

Jordan, D.B., Ogren, W.L.: The CO₂/O₂ specificity of ribulose 1,5-bisphosphate carboxylase/oxygenase. Dependence on ribulosebisphosphate concentration, pH and temperature. – *Planta* **161**: 308-313, 1984.

Joshi, S.C., Palni, L.M.S.: Greater sensitivity of *Hordeum himalayens* Schult. to increasing temperature causes reduction in its cultivated area. – *Curr. Sci.* **89**: 879-882, 2005.

June, T., Evans, J.R., Farquhar, G.D.: A simple new equation for the reversible temperature dependence of photosynthetic electron transport: a study on soybean leaf. – *Funct. Plant Biol.* **31**: 275-283, 2004.

Larcher, W.: *Physiological Plant Ecology*. – Springer, Berlin 2003.

Leuning, R.: A critical appraisal of a combined stomatal-photosynthesis model for C₃ plants. – *Plant Cell Environ.* **18**: 339-355, 1995.

Leuning, R.: Scaling to a common temperature improves the correlation between the photosynthetic parameters J_{\max} and $V_{c\max}$. – *J. exp. Bot.* **48**: 345-347, 1997.

Lichtenthaler, H.K.: Chlorophylls and carotenoids – pigments of photosynthetic biomembranes. – In: Colowick, S.P., Kaplan, N.O. (ed.): *Methods in Enzymology*. Vol. 148. Pp. 350-382. Academic Press, San Diego – New York – Berkeley – Boston – London – Sydney – Tokyo – Toronto 1987.

Makino, A., Mae, T.: Photosynthesis and plant growth at elevated levels of CO₂. – *Plant Cell Physiol.* **40**: 999-1006, 1999.

Marek, M., Pirochová, M.: Response of the ratio of intercellular CO₂ concentration to ambient CO₂ concentration (C_i/C_a-ratio) to basic microclimatological factors in an oak-hornbeam forest. – *Photosynthetica* **24**: 122-129, 1990.

Prioul, J.L., Chartier, P.: Partitioning of transfer and carboxylation components of intercellular resistance to photosynthetic CO₂ fixation: A critical analysis of the methods used. – *Ann. Bot.* **41**: 789-900, 1977.

Reich, P.B., Ellsworth, D.S., Walters, M.B.: Leaf structure (SLA) modulates photosynthesis relations: evidence from within and across species, functional groups and biomes. – *Funct. Ecol.* **12**: 948-958, 1998.

Salvucci, M.E., Crafts-Brandner, S.J.: Mechanisms for deactivation of Rubisco under moderate heat stress. – *Physiol. Plant.* **122**: 513-519, 2004.

Wohlfahrt, G., Bahn, M., Haubner, E., Horak, I., Michaeler, W., Rottmar, K., Tappeiner, U., Cernusca, A.: Inter-specific variation of the biochemical limitation to photosynthesis and related leaf traits of 30 species from mountain grassland ecosystems under different land use. – *Plant Cell Environ.* **22**: 1281-1296, 1999.

Wullschleger, S.D.: Biochemical limitations to carbon assimilation in C₃ plants – A retrospective analysis of the A/C_i curves from 109 species. – *J. exp. Bot.* **44**, 907-920, 1993.

Xu, L.K., Hsiao, T.C.: Predicted versus measured photosynthetic water-use efficiency of crop stands under

dynamically changing field environments. – *J. exp. Bot.* **55**: 2395-2411, 2004.

Yamasaki, T., Yamakawa, T., Yamane, Y., Koike, H., Satoh, K., Katoh, S.: Temperature acclimation of photosynthesis and related changes in photosystem II electron transport in winter wheat. – *Plant Physiol.* **128**: 1087-1097, 2002.

Zhang, S., Li, Q., Ma, K., Chen, L.: Temperature-dependent gas exchange and stomatal/non-stomatal limitation to CO_2 assimilation of *Quercus liaotungensis* under midday high irradiance. – *Photosynthetica* **39**: 383-388, 2001.

ERRATUM

M.A. El-Sharkawy: International research on cassava photosynthesis, productivity, eco-physiology, and responses to environmental stresses in the tropics. – *Photosynthetica* 44: 481-512, 2006.

Please correct the equations in Fig. 3C on p. 485 as follows:

for the humid environments $\text{WUE} = 1.57 + 9.9/\text{VPD}$

for the seasonally dry environments $\text{WUE} = 1.06 + 18.9/\text{VPD}$

for the semi-arid environments $\text{WUE} = 0.69 + 24.3/\text{VPD}$

The publisher and author apologize for these errors and for inconveniences it may have caused.